High Resolution Infrared Spectroscopy of the CO_2-Br_2 Weakly Bound Complex

A. Sazonov and R. A. Beaudet*

Department of Chemistry, University of Southern California, University Park,
Los Angeles, California 90089-0482

Received: September 30, 1997; In Final Form: January 27, 1998

The absorption spectrum of the weakly bound complex CO_2-Br_2 has been observed by probing the asymmetric stretch of the CO_2 moiety near 2349 cm^{-1}. The complex was formed by the supersonic expansion of a mixture of CO_2 and bromine vapor with He as a carrier gas. CO_2-Br_2 was found to have a linear structure with one Br atom close to the center of mass of the system. The isotopic mixture of the second Br provided the splitting of the observed peaks into two. The measured rotational and distortion constants for ^{79}Br and ^{81}Br are $B' = 0.0148044(26)$, $D' = 6.43(17) \times 10^{-8}$, $B'' = 0.0146591(26)$, $D'' = 6.01(16) \times 10^{-8}$ and $B' = 0.0146763(27)$, $D' = 6.42(18) \times 10^{-8}$, $B'' = 0.0145321(28)$, $D'' = 6.04(19) \times 10^{-8}$, respectively (in cm^{-1}). The distances from the Br_2 bond center to the C atom are 5.116 and 5.083 Å for the ground and excited states, respectively, and the force constant of the van der Waals stretching mode is estimated to be 0.004 mdyn/Å in both states. The experimental values are compared with the results of ab initio calculations performed at the Hartree−Fock and MP2 levels. The origin of van der Waals binding between CO_2 and Br_2 and the floppiness of the complex are discussed.

1. Introduction

Diode laser infrared (IR) spectroscopy has proven to be an effective method for studying weakly bound complexes,[1] and carbon dioxide complexes are a natural choice for such studies. The asymmetric stretch normal mode has one of the largest transition dipole moments. Also, because CO_2 has been used in a number of oriented-reactant experiments, it is desirable to characterize the weakly bound precursors as fully as possible.[2,3]

To date, high-resolution rovibrational spectroscopy has provided the structures and vibrational dynamics of a wide variety of CO_2 weakly bound complexes. Here we will only review those that are pertinent to our study. The following trends have been observed in CO_2−rare gas (Rg) series of complexes (Rg = He−Xe): (i) the distance between C and the RG atom increases monotonically whereas the mean value of the angle between the C−Rg and CO_2 axes approaches 90° in going from Ne to Xe; (ii) the CO_2 asymmetric stretch band origin, ν_3, shifts to lower frequencies.[4] However, as was shown later,[5] in the CO_2−He complex, the internuclear distance R(He−C) = 3.58 Å is surprisingly greater than R(Ne−C) = 3.30 Å in the CO_2−Ne complex. Such an exception can be caused by two factors. First, because the He atom has only two electrons, van der Waals attraction between the species should be extremely weak and repulsive forces may start to contribute significantly at longer separations. Second, due to its small mass and weak binding, the He atom can undergo large amplitude zero point motions leading to an observed distance that does not reflect the minimum of the potential well (even approximately).

The CO_2−H(D)X (X = F, Cl, Br) complexes have also been extensively studied by rotational and rovibrational spectroscopy. Linear equilibrium geometries were observed for HF, HCl and the corresponding deuterides.[6−10] For HF and HCl, the CO_2 asymmetric stretch band origins, ν_3, were blue-shifted by 9.9 and 3.9 cm^{-1}, respectively, and deuteration resulted in larger blue shifts of 10.6 and 4.7 cm^{-1}, respectively. On the other hand, the CO_2−H(D)Br structure was found to be inertially T-shaped (R_{cm} = 3.58 Å), with essentially parallel HBr and CO_2 axes. The ν_3 rovibrational band origin was red-shifted by 0.94 and 0.87 cm^{-1} for HBr and DBr, respectively.[11] The microwave spectra of eight HBr−CO_2 isotopomers[12] are consistent with a T-shaped Br−CO_2 geometry giving, however, an equilibrium CBrH angle of ≈ 103° (versus 86° as obtained by Zeng et al.[11]).

Only a few studies on Br_2 complexes have been reported. Fluorescence excitation spectra associated with the Br_2(B ← X) bands in He−Br_2[13] and Ne−Br_2[14,15] have been recorded and their rotational structure has been resolved. Both complexes have a T-shaped geometry with the separation between the noble gas atom and the Br_2 bond center of R_{cm} = 3.7 and 3.65 Å for He and Ne, respectively.

Bloemink and Legon[16] investigated the ground states of four isotopomers of the prereactive intermediate $H_3N\cdots Br_2$ with Fourie transform microwave spectroscopy. Chemical reaction between the monomers was avoided by using a fast-mixing nozzle. The symmetric-top spectra were analyzed to determine rotational constants, the centrifugal distortion constants D_J and D_{JK}, the Br nuclear quadrupole coupling constants for both bromine atoms, and the Br nuclear spin-rotation coupling constants. The distances r (N$\cdots$Br$_{\text{inner}}$) = 2.72(2) Å and r (Br−Br) = 2.335(10) Å in the complex were obtained from the rotational constants, and the intermolecular stretching force constant k_σ = 18.5(5) N m^{-1} was estimated from D_J.

High-resolution rovibrational absorption spectra of OC−Br_2[17] have been recorded in the region of the CO stretching mode near 2143 cm^{-1}. Four progressions originating from different bromine isotopic species were consistent with a linear complex. The distances from the Br_2 bond center to the CO center of mass were 4.884 and 4.893 Å for the ground and excited states, respectively. The orientation of CO was presumed to be the same as in CO−Cl_2. In Bunte's studies of the OC−Cl_2 complex, a good agreement between ab initio calculated[18] and experimentally measured[19] spectroscopic constants was obtained.

S1089-5639(97)03163-0 CCC: $15.00

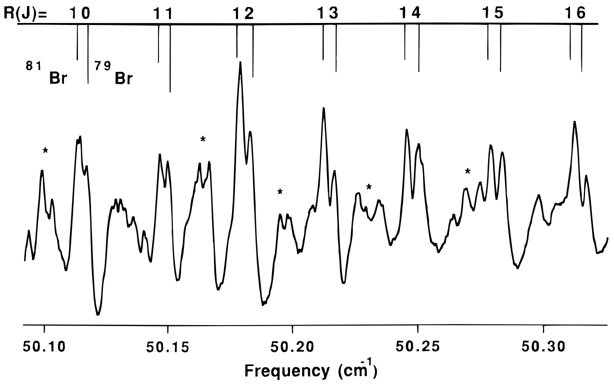

Figure 1. A portion of the R branch of the $CO_2{-}Br_2$ $\nu_{3CO_2} = 0 \rightarrow 1$ spectrum. The peaks marked with an asterisk are assigned to $(CO_2)_2$.

The ab initio results suggested that the equilibrium structure of that complex is $OC{-}Cl_2$. The later microwave study of seven isotopic species of $OC{-}Cl_2$[20] has shown the same result. Based on the simple analogy and supported by the Lewis acid−base model of the binding for the carbonyl group in complexes, the $OC{-}Br_2$ structure was proposed; however, neither ab initio calculations nor microwave studies of this molecule have been performed yet.

In this work, we report the rovibrational absorption spectrum of the $CO_2{-}Br_2$ weakly bound complex observed by pulsed-nozzle, diode laser IR spectroscopy.

2. Experimental Setup

The detailed experimental setup has been described previously,[21] and only a few aspects relevant to this particular study are presented below. A mixture of ≈0.2% CO_2 and ≈0.8% Br_2 (Mallinckrodt, 99.7% of bromine) in He was expanded through a pulsed slit nozzle at a rate of 3 Hz from a stagnation pressure of ≈2 atm. Background pressure in the chamber was ∼10 mTorr during the expansion. Each gas pulse lasted 1.5 ms. A single mode from a tunable IR diode laser (operating near 2349 cm^{-1}, which corresponds to the asymmetric stretching mode of CO_2) was selected by a 0.5-m monochromator. Two small fractions of the diode power were sent through a CO_2 reference gas cell and a confocal Etalon (FSR = 0.099 cm^{-1}) to calibrate the frequency scale. Most of the laser radiation entered the vacuum chamber and made a double pass through the gas expansion space. All three IR absorption signals were taken simultaneously by rapidly scanning the laser frequency during a stable period of the gas pulse. The supersonic jet absorption signal was filtered through a band-pass filter, which cut off the frequencies outside the range 10−100 kHz. The diode laser was scanned ∼0.35 cm^{-1} during each gas pulse and usually 100 scans were averaged. The absorption features presumably belonging to the $CO_2{-}Br_2$ complex were recorded between 2347.5 and 2351.5 cm^{-1}. These absorptions were not present when either of the two components (CO_2, Br_2) was absent. However, some peaks belonging to the CO_2 dimer were observed. The gas concentrations were adjusted to obtain the strongest spectrum while minimizing the $(CO_2)_2$ resonances.

3. Spectral Analysis

The observed spectrum can be divided into two portions. Figure 1 displays a small portion of the high-frequency region. These transitions were only observed when bromine was present in the expansion gas mixture. Thus, we conclude that this spectrum belongs to a complex containing bromine. The lines are broadened by the unresolved nuclear quadrupole hyperfine splittings which is usually more preponderant for low *J* transitions. Some peaks here were identified to belong to the $\nu_3 = (1 \leftarrow 0)$ rovibrational band of $(CO_2)_2$. It was not possible to completely rid the spectrum of CO_2 dimer transitions. However, the most prominent feature of this spectrum is a progression of lines equally separated by ≈0.034 cm^{-1}, degraded to the higher frequencies, and split into doublets of equal intensity. Because no other series with similar spacing was found, it was concluded that the complex must have linear or quasilinear geometry. Because naturally occurring bromine contains two isotopic species, ^{79}Br and ^{81}Br, in nearly equal proportion, (50.54% and 49.46%, respectively), we would expect that the spectrum should consist of equally intense quadruplets, one line for each of the four possible isotopomers ($CO_2{-}{}^{79}Br^{79}Br$, $CO_2{-}{}^{81}Br^{79}Br$, $CO_2{-}{}^{79}Br^{81}Br$, and $CO_2{-}{}^{81}Br^{79}Br$). However, as confirmed later, the inner bromine is nearly at the center of mass (cf. Table 2), and the isotopic splitting between the isotopomers with different inner bromines could not be resolved. During the review of this manuscript, one reviewer had serious concern that the spectrum was not a simple $\Sigma{-}\Sigma$ transition, but a $\Pi{-}\Pi$ transition with splittings due to l-doubling. However, if this were the case, we would still expect to observed two spectrally resolved isotopomers of equal intensity, thus quartets or octets and not doublets.

In summary, the observed splittings must be attributed to the presence of different isotopically substituted species with the inner Br atom situated *very close* to the center of mass of the complex. These species will hence be denoted $CO_2{-}{}^{79}Br_2$ and $CO_2{-}{}^{81}Br_2$, where the superscript denotes the mass number of the outer Br.

The measured transition frequencies of the two isotopomers were fit to the semirigid linear rotor model,

$$\nu = \nu_0 + B'J'(J'+1) - D'(J'(J'+1))^2 - B''J''(J''+1) + D''(J''(J''+1))^2$$

where all terms have their usual meanings. The experimental and calculated frequencies are listed in Table 1 (blended lines were not included into the fit and are not reported). The spectroscopic constants are given in Table 2. Because the addition of higher order centrifugal distortion terms did not improve the fit, they were omitted. After the simulation of the entire spectrum, the rotational temperature of the formed complex was estimated to be 7 ± 1 K.

Assuming that the internuclear distances in CO_2 and Br_2 remain the same upon complexation, the distance between centers of mass of the monomers can be expressed as follows:

$$R_{cm} = \sqrt{\frac{I_{complex} - I_{CO_2} - I_{Br_2}}{\mu}}$$

where *I*s are the corresponding moments of inertia and μ is the reduced mass of the binary complex. Mass of the inner bromine was set equal to 79 or 81 amu for both experimentally distinguished isotopomers. Thus, the four values of R_{cm} were calculated. The isotopic shift of the center of mass position in Br_2,

$$\Delta R = R_{Br_2} \frac{m_{inner} - m_{outer}}{2(m_{inner} + m_{outer})}$$

TABLE 1: Experimental and Calculated Transition Frequencies of the CO_2-Br_2 Complex[a]

transition	($CO_2-^{79}Br_2$)	($CO_2-^{81}Br_2$)	transition	($CO_2-^{79}Br_2$)	($CO_2-^{81}Br_2$)
P(3)	2349.6888(−0)	2349.6895(+1)	R(1)	2349.8353(−1)	
P(4)	2349.6603(+0)	2349.6610(−2)	R(2)	2349.8659(+3)	2349.8647(−0)
P(5)	2349.6328(+6)	2349.6332(−2)	R(3)	2349.8966(+6)	2349.8948(−1)
P(6)	2349.6043(−1)	2349.6057(−1)	R(5)	2349.9578(−1)	2349.9561(+0)
P(7)	2349.5768(−1)	2349.5784(−1)	R(6)	2349.9889(−3)	2349.9874(+2)
P(8)	2349.5496(+1)	2349.5513(−1)	R(7)	2350.0204(−3)	2350.0189(+4)
P(9)	2349.5228(+2)	2349.5247(+0)	R(8)	2350.0522(−4)	2350.0503(+2)
P(10)	2349.4956(−3)	2349.4984(+1)	R(9)	2350.0848(+1)	2350.0816(−4)
P(11)	2349.4695(−1)	2349.4721(−1)	R(10)	2350.1171(−1)	2350.1146(+4)
P(12)	2349.4436(−0)	2349.4462(−2)	R(11)	2350.1499(+0)	2350.1467(+1)
P(13)	2349.4176(+2)	2349.4211(+2)	R(12)	2350.1830(+2)	2350.1791(−2)
P(14)	2349.3923(−1)	2349.3956(−1)	R(13)	2350.2167(+7)	2350.2124(+3)
P(15)	2349.3677(+5)	2349.3705(−2)	R(14)	2350.2498(+3)	2350.2457(+3)
P(16)	2349.3417(−7)	2349.3457(−4)	R(15)	2350.2836(+4)	2350.2790(+3)
P(17)	2349.3177(−1)	2349.3217(−2)	R(16)	2350.3171(−1)	2350.3124(−0)
P(18)	2349.2936(−0)	2349.2975(−3)	R(17)	2350.3510(−2)	2350.3463(−2)
P(19)	2349.2696(−1)	2349.2747(+6)	R(18)	2350.3856(−3)	2350.3807(+2)
P(20)	2349.2461(−0)	2349.2503(−4)	R(19)	2350.4203(−3)	2350.4151(−0)
P(21)	2349.2221(−7)	2349.2281(+6)	R(20)	2350.4555(−1)	2350.4496(−1)
P(22)	2349.1998(+1)	2349.2049(+2)	R(21)	2350.4906(−2)	2350.4845(−1)
P(23)	2349.1769(−1)	2349.1824(+2)	R(22)	2350.5260(−2)	2350.5190(−7)
P(24)	2349.1548(+3)	2349.1605(+4)	R(23)	2350.5615(−4)	2350.5550(−2)
P(25)	2349.1328(+5)	2349.1385(+4)	R(24)	2350.5973(−4)	2350.5903(−5)
P(26)	2349.1101(−5)	2349.1165(−0)	R(25)	2350.6264(−2)	
P(27)	2349.0896(+7)	2349.0948(−4)	R(26)	2350.6706(+4)	2350.6627(+1)
P(28)	2349.0680(+3)	2349.0737(−4)	R(27)	2350.7071(+4)	2350.6994(+6)
P(29)	2349.0470(+2)	2349.0533(−1)	R(28)	2350.7438(+3)	2350.7354(+1)
P(30)	2349.0263(+2)	2349.0331(+2)	R(29)	2350.7807(+2)	
P(31)	2349.0057(−1)	2349.0134(+6)	R(30)	2350.8178(+2)	2350.8088(+0)
P(32)	2348.9857(−1)	2348.9927(−2)	R(31)	2350.8548(−2)	2350.8461(+1)
P(33)	2348.9659(+1)	2348.9730(−3)	R(32)	2350.8921(−5)	2350.8830(−2)
P(34)	2348.9461(−2)		R(33)	2350.9305(+2)	2350.9209(+2)
P(36)	2348.9079(−3)				

[a] Residuals in parentheses are from the least-squares fit and are (observed − calculated) × 10^{-4}; $\sigma = 0.0003$ cm^{-1}.

TABLE 2: Molecular Constants of the CO_2-Br_2 Complex[a]

molecular constant	$CO_2-^{79}Br_2$	$CO_2-^{81}Br_2$
ν_0 (cm^{-1})	2349.775866(89)	2349.775770(95)
B'' (cm^{-1})	0.0146591(26)	0.0145321(28)
B' (cm^{-1})	0.0148044(26)	0.0146763(27)
I'' (amu-Å ± 2)	1149.97(20)	1160.03(20)
I' (amu-Å ± 2)	1138.71(20)	1148.65(20)
D'' (cm^{-1})	$6.01(16) \times 10^{-8}$	$6.04(19) \times 10^{-8}$
D' (cm^{-1})	$6.43(17) \times 10^{-8}$	$6.42(18) \times 10^{-8}$
R_0'' (Å)	5.1161(6)	5.1160(6)
R_0' (Å)	5.0830(6)	5.0828(6)
ω'' (cm^{-1})	14.5(2)	14.3(2)
ω' (cm^{-1})	14.2(2)	14.0(2)
$R_{OBr''}$ (Å)	2.8118(6)	2.8117(6)
R_{OBr}' (Å)	2.7797(6)	2.7795(6)
k_σ'' (mdyn/Å)	0.0043(1)	0.0042(1)
k_σ' (mdyn/Å)	0.0041(1)	0.0040(1)

[a] Uncertainties are in the last two digits and are one standard deviation of least-squares fit.

was then taken into account and the isotopically invariant distance between geometric centers of the monomers $R_0 = R_{cm} + \Delta R$ was eventually calculated. Within the experimental error, the R_0 values were not affected by the mass of the inner Br.

We also confirmed our results by calculating the coordinates of all atoms in the center of mass coordinate system after fitting R_{cm} to the rotational constants. These results are given in Table 3. The inner bromine coordinates are −0.028 Å and −0.050 Å for $CO_2-^{79}Br_2$ and $CO_2-^{81}Br_2$, respectively, which causes respective isotopic shifts in the moment of inertia of 0.001 and 0.005 amu-Å^2, which arewell beyond our experimental accuracy.

With the use of the pseudo-diatomic approximation, van der Waals stretching vibrational frequencies were obtained as follows:[22]

$$\omega = \sqrt{\frac{4B^3}{D}}$$

whereupon the force constants for both states, were evaluated:

$$k_\sigma = \mu\omega^2$$

The molecular constants are given in Tables 2 and 3.

4. Ab Initio

The Hartree−Fock self-consistent field (HF) technique along with the Møller−Plesset many body second-order perturbation theory (MP2) were used to calculate the van der Waals potential energy surface (PES) for the CO_2-Br_2 system. Commonly employed 6-31+g* basis sets[23] ($\zeta_d = 0.8$) were used for carbon and oxygen. To describe bromine, a compact valence double-ζ Gaussian-type basis set developed by Andzelm et al.,[24] augmented with two sets of *d*-polarization functions ($\zeta_d = 0.562$, 0.176), was used because it reproduces the molecular properties of Br_2. For equilibrium structures, both van der Waals and intramolecular parameters were optimized. Basis set superposition error (BSSE) was accounted for by the counterpoise method.[25] The calculations were performed using *Gaussian-92*.[26]

The three distinct minima, linear, parallel, and nonplanar X-shaped, were found on the CO_2-Br_2 PES when either level of theory was used. In Figure 2 the MP2 energies for all three equilibrium structures are plotted as a function of R_{cm}. The calculated molecular parameters of these isomers are listed in Table 4. In all three cases, including MP2 corrections shortens the equilibrium R_{cm}, suggesting a significant contribution of

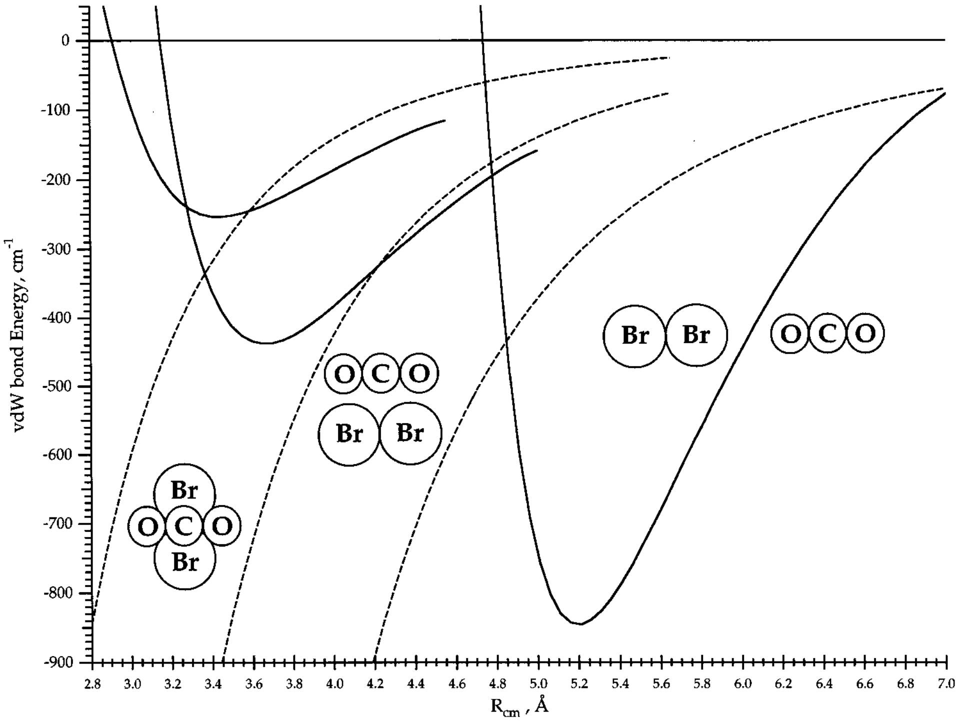

Figure 2. Ab initio calculated equilibrium geometries of the CO_2−Br_2 complex and potential energies along the R_{cm} distances. Calculations were done at the MP2 level and corrected for BSSE. Dashed lines represent the quadrupole−quadrupole potential, V_{qq} (see section 5 for the details).

TABLE 3: Atomic Coordinates (Å) of the Atoms and *R*(O−Br) in the CO_2−Br_2 Complex[a]

	atomic coordinates (Å)			
atom	CO_2−$^{79}Br^{79}Br$	CO_2−$^{81}Br^{79}Br$	CO_2−$^{79}Br^{81}Br$	CO_2−$^{81}Br^{81}Br$
ground state				
O	−5.1634	−5.1632	−5.1855	−5.1850
C	−4.0014	−4.0012	−4.0235	−4.0230
O	−2.8394	−2.8392	−2.8615	−2.8610
Br	−0.0277	−0.0274	−0.0498	−0.0493
Br	+2.2563	+2.2566	+2.2342	+2.2347
excited state				
O	−5.1384	−5.1382	−5.1602	−5.1596
C	−3.9764	−3.9762	−3.9982	−3.99766
O	−2.8144	−2.8142	−2.8362	−2.8356
Br	−0.0346	−0.0344	−0.0568	−0.0562
Br	+2.2493	+2.2495	+2.2272	+2.2278
fitted distance				
R″(O−Br)	2.8118	2.8118	2.8117	2.8117
R′(O−Br)	2.7797	2.7797	2.7795	2.7795

[a] Assumes r(CO) = 1.162 Å and R(Br−Br) = 2.290 Å. R(O−Br) was calculated by fitting this distance to the moments of inertia with the correct isotopic masses.

electron correlation to the van der Waals bond energy. The MP2 calculated R_{cm} for the linear isomer (5.227 Å) agrees with the experimental value (5.116 Å). The small discrepancy can arise from the underestimation of a total configuration interaction by MP2. The HF calculation of vibrational frequencies leads to an incorrect large value for $\Delta\nu_3(CO_2)$ (8.1 instead of 0.6 cm^{-1}) and to an overestimated van der Waals stretch frequency (49 cm^{-1} by ab initio versus 14 cm^{-1} estimated from the centrifugal distortion constant). Because of limited computer resources, the MP2 vibrational frequencies were not been calculated.

5. Discussion

As shown in the previous section, the experimentally observed linear CO_2−Br_2 is predicted to have the lowest energy among all its isomers. Neither the parallel nor the X-shaped structures were observed. Because the height of the barriers between linear and nonlinear structures were not determined, there is no reason to believe that these other forms actually exist. Also, because of the low temperature created by supersonic expansion, the concentration of the higher energy forms should be small if an equilibrium is attained.

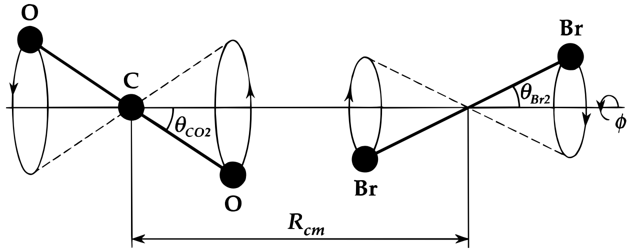

Figure 3. The structure of CO_2−Br_2 and the definition of the coordinates.

Although ab initio calculations can, in principle, explain the structures of CO_2−Br_2 (in terms of molecular orbitals), it is intuitively more meaningful to apply a simple electrostatic model. The first nonvanishing term in the multipole expansion for CO_2−Br_2 is the quadrupole−quadrupole interaction:

$$V_{QQ} = \frac{3Q_{CO_2}Q_{Br_2}}{4R_{cm}^5}[1 - 5\cos^2\theta_{CO_2} - 5\cos^2\theta_{Br_2} + 17\cos^2\theta_{CO_2}\cos^2\theta_{Br_2} + 2\sin^2\theta_{CO_2}\sin^2\theta_{Br_2}\cos^2\phi - 16\sin\theta_{CO_2}\sin\theta_{Br_2}\cos\theta_{CO_2}\cos\theta_{Br_2}\cos\phi]$$

where Q_{CO_2} and Q_{Br_2} are the permanent quadrupole moments of the monomers, and the definition of coordinates is given in Figure 3.[27] We will now only consider angular coordinates while R_{cm} remains constant.

In general, the shape of the quadrupole−quadrupole potential is determined by the signs of the quadrupole moments of the

TABLE 4: Ab Initio Results and Molecular Constants of CO_2−Br_2 Complex

molecular constant	HF	MP2	HF	MP2	HF	MP2
R_{cm} (Å)	5.4931	5.2272	4.1926	3.6532	3.9439	3.3271
θ_{CO_2} (°)	0	0	90	90	90	90
θ_{Br_2} (°)	0	0	90	90	90	90
ϕ (°)	—	—	0	0	90	90
R_{CO} (Å)[a]	1.1433 (+0)	1.1817 (+9)	1.1435 (+2)	1.1820 (+12)	1.1435 (+2)	1.1819 (+11)
R_{BrBr} (Å)[a]	2.2919 (+10)	2.3186 (+33)	2.2920 (+11)	2.3184 (+31)	2.2930 (+21)	2.3176 (+23)
E_{vdW} (cm^{-1})	−577	−845	−191	−437	−169	−277
$\nu_{3(CO_2)}$ (cm^{-1})[b]	2572.71 (+8.10)		2569.21 (+4.60)		2569.75 (+5.14)	
$\nu_{1(CO_2)}$ (cm^{-1})[b]	1513.51 (+2.38)		1511.41 (+0.28)		1511.40 (+0.27)	
$\nu_{2(CO_2)}$ (cm^{-1})[b,c]	753.75(+4.42)		753.57 (+4.24)		752.14 (+2.81)	
	—		751.81 (+2.48)		750.37 (+1.04)	
$\nu_{(Br_2)}$ (cm^{-1})[b]	337.18 (+0.74)		336.13 (−0.31)		334.93 (−1.51)	
ω_{1vdW} (cm^{-1})[d]	54.74 (Π)		24.57 (A_1)		22.44 (A_1)	
ω_{2vdW} (cm^{-1})[d]	49.16 (Σ)		24.39 (B_2)		21.04 (B_2)	
ω_{3vdW} (cm^{-1})[d]	20.29 (Π)		7.22 (A_2)		8.85 (B_1)	
ω_{4vdW} (cm^{-1})[d]	—		5.36 (B_2)		4.43 (A_2)	

[a] Change with respect to free monomer [e.g., *r*(complex) − *r*(free), in Å × 10^{-4}] is in parentheses. [b] Shift with respect to free monomer [e.g., ν(complex) − ν(free), in cm^{-1}] is in parentheses. [c] $\nu_{2(CO_2)}$ is split in the nonlinear isomers. [d] Symmetry is in parentheses.

partners. For two quadrupoles of the same sign, it has two minima, corresponding to two T-shaped structures, isoenergetic at the same R_{cm}. A saddle point of first order corresponds to a slipped parallel geometry with the slipping angle ~50°. The analysis of the potential for the case of two quadrupoles of opposite sign leads to two minima corresponding to the linear and the parallel isomers. A saddle point of first order occurs for the X-shaped geometry. The ratio between the energies of those three structures (at constant R_{cm}) is 8:3:1; the most stable one is linear and the least stable one is X-shaped.

The estimated quadrupole−quadrupole contributions, V_{qq}, for CO_2−Br_2 are represented by dashed lines in Figure 2. The experimental value of $Q_{CO_2} = -14.34 \times 10^{-40}$ cm^2 was used.[28] The value of $Q_{Br_2} = 30.52 \times 10^{-40}$ cm^2 was taken from ab initio calculations;[29] the experimental value of Q_{Br_2} has not been reported. In comparison with the ab initio results, the V_{qq} values reflect the same trend in energy. Based on this result the absolute and relative stabilities of the linear and parallel isomers can be explained primarily by an electrostatic origin. In the case of an X-shaped isomer, the repulsion between O and Br atoms should be much smaller than in the parallel isomer case. This over repulsion allows the monomers to approach closer, so close that the forces other than quadrupole−quadrupole provide a minimum with respect to the ϕ angle. A stable X-shaped structure is now found for the CO_2−CS_2 van der Waals complex.[30] A similar mechanism is probably also responsible for slipped parallel equilibrium geometries of the homomolecular dimers $(CO_2)_2$[31] and $(N_2O)_2$,[32] and the heteromolecular dimer CO_2−N_2O.[21]

The spectroscopic study of linear CO_2−Br_2 suggests a significant (~0.033 Å) contraction of the van der Waals bond with vibrational excitation of CO_2. An analogous effect has been observed in a number of IR studies of weakly bound complexes.[6,10] For example, in CO_2−H(D)F, such a contraction takes place when either the H(D)F stretch or CO_2 asymmetric stretch vibrations is excited. It is known that the r_{CO} distance in the $\nu_3 = 1$ CO_2 is lengthened by ~0.0022 Å with respect to that in the ground state[33] (it was taken into account when we calculated R'_{cm}). This change is expected to increase the value of Q_{CO_2} and, consequently, the attraction between the monomers. Moreover, both molecules must induce small dipole moments in partners that give rise to an intermolecular attraction, and these moments are also dependent on r_{CO}.

Finally, an additional computer experiment was performed; that is, the CO distances in the linear complex were raised by 0.0022 Å and kept fixed while other parameters (R_{cm} and R_{BrBr}) were allowed to vary. The result of an optimization done by this expedient on the HF level was the decrease of R_{cm} by 0.05 Å, which supports our interpretation of the effect.

Surprisingly, the intermolecular stretch force constant is not affected by the excitation of CO_2, only a little softening of this mode (within the experimental error for both isotopomers) can be obtained. In contrast to the present study, drastic decreases in k_σ were observed in CO_2−H(D)F, SCO−HF, and other linear complexes. It is interesting to note that in such systems, the softening of van der Waals stretching is accompanied by the decrease of van der Waals molecular radii already mentioned, and the conclusions about stabilization or destabilization of the intermolecular bonds on excitation are then ambiguous. There is no escape from the fact that the experimentally determined stretching force constants of CO_2−Br_2 are anomalously weak even for a van der Waals bond.

Up to this point we have considered a real CO_2−Br_2 system in terms of a rigid distortable molecule. It is also worth turning to the alternative model of a floppy linear rotor,[34] which is extensively used in microwave studies.[16,35] Here the contribution of intermolecular bending vibrations to the zero-point motion of the complex is described by the oscillating angles θ_{CO_2}, θ_{Br_2} and ϕ (see Figure 3), so that the moment of inertia of the complex is given by:

$$\langle I\rangle \approx \mu\langle {R_{cm}}^2\rangle + I_{CO_2}\left\langle\frac{1+\cos^2\theta_{CO_2}}{2}\right\rangle + I_{Br_2}\left\langle\frac{1+\cos^2\theta_{Br_2}}{2}\right\rangle$$

where the angular brackets indicate the average over the zero-point motion. One can see that if $\langle\cos^2\theta_{CO_2}\rangle$ and/or $\langle\cos^2\theta_{Br_2}\rangle$ differ from 1, the actual $\langle R_{cm}\rangle$ is somewhat longer than that determined for a rigid rotor. As calculated ab initio, the intermolecular potential (Figure 4) does not allow monomers to oscillate about the equilibrium point with a large amplitude. Unfortunately, there is no way to obtain all three values of interest from only two experimentally measured rotational constants of isotopomers without additional assumptions. The only thing one must keep in mind is that the experimental values of R_{cm} reported in this work are actually lower limits of the corresponding molecular parameters.

In summary, we have obtained and assigned the ν_3 band of CO_2−Br_2 in terms of a semirigid linear rotor Hamiltonian. The structure in the ground and excited vibrational states has been accurately determined. The linear equilibrium geometry and a

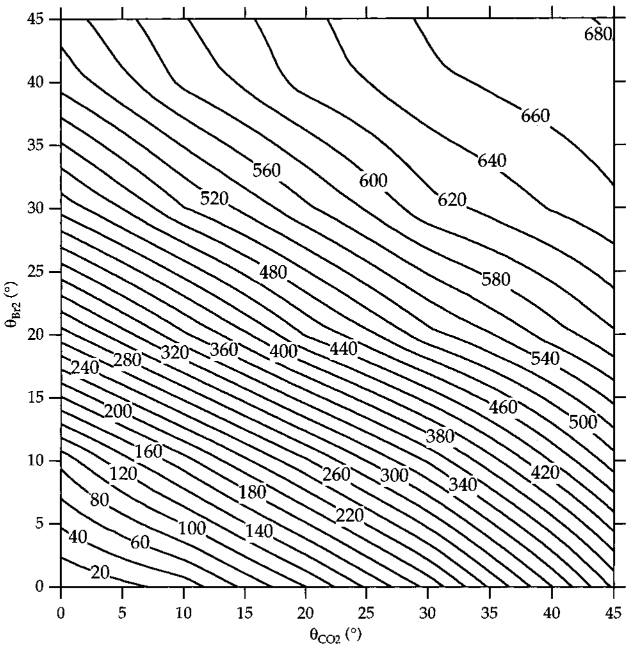

Figure 4. Potential contours for the linear CO_2-Br_2 as a function of θ_{CO_2} and θ_{Br_2}. Calculations were done at the MP2 level and corrected for BSSE. Contour spacing is 20 cm^{-1}. Zero corresponds to the energy of the equilibrium structure (see Table 4).

small shift of the vibrational frequency in the chromophore imply that the van der Waals binding mechanism in the CO_2-Br_2 complex is predominantly electrostatic.

Acknowledgment is made to the donors of the Petroleum Research Fund, administered by the American Chemical Society, for the partial support of this research and for the support of the U.S. Army Research Office under the auspices of the Center for the Study of Fast Transient Processes under grant number DAAL03-92-G-0175. We gratefully acknowledge Dr. Terry Miller for his SPECSIM spectral simulation program and Dr. Herb Pickett who provided us with his SPIN programs. We also thank Dr. Steve Bunte for computational time on his Silicon Graphics computer, "Fight on!"

References and Notes

(1) Miller, R. E. In: *Atomic and Molecular Beam Methods*, vol. 2; Scoles, G., Ed.; Oxford University: New York, 1992; pp 192−212.

(2) Buelow, S.; Noble, M.; Radhakrishnan, G.; Reisler, H.; Wittig, C.; Hancock, G. *J. Phys. Chem.* **1986**, *90*, 1015.

(3) Buelow, S.; Radhakrishnan, G.; Wittig, C. *J. Phys. Chem.* **1987**, *91*, 5409.

(4) Randall, R. W.; Walsh, M. A.; Howard, B. J. *Faraday Discuss. Chem. Soc.* **1988**, *85*, 13.

(5) Weida, M. J.; Sperhac, J. M.; Nesbitt, D. J. *J. Chem. Phys.* **1994**, *101*, 8351.

(6) Fraser, G. T.; Pine, A. S.; Suenram, R. D.; Dayton, D. C.; Miller, R. E. *J. Chem. Phys.* **1989**, *90*, 1330.

(7) Lovejoy, C. M.; Schuder, M. D.; Nesbitt, D. J. *J. Chem. Phys.* **1987**, *86*, 5337.

(8) Baiocchi, F. A.; Dixon, T. A.; Joyner, C. H.; Klemperer, W. *J. Chem. Phys.* **1981**, *74*, 6544.

(9) Altman, R. S.; Marshall, M. D.; Klemperer, W. *J. Chem. Phys.* **1982**, *77*, 4344.

(10) Sharpe, S. W.; Zeng, Y. P.; Wittig, C.; Beaudet, R. A. *J. Chem. Phys.* **1990**, *92*, 943.

(11) Zeng, Y. P.; Sharpe, S. W.; Shin, S. K.; Wittig, C.; Beaudet, R. A. *J. Chem. Phys.* **1992**, *97*, 5392.

(12) Rice, J. K.; Lovas, F. J.; Fraser, G. T.; Suenram, R. D. *J. Chem. Phys.* **1995**, *103*, 3877.

(13) van de Burgt, L. J.; Nicolai, J.-P.; Heaven, M. C. *J. Chem. Phys.* **1984**, *81*, 5514.

(14) Swartz, B. A.; Brinza, D. E.; Western, C. M.; Janda, K. C. *J. Phys. Chem.* **1984**, *88*, 6272.

(15) Thommen, F.; Eward, D. D.; Janda, K. C. *J. Chem. Phys.* **1985**, *82*, 5295.

(16) Bloemink, H. I.; Legon, A. C. *J. Chem. Phys.* **1995**, *103*, 876.

(17) Lin, Y.; Beaudet, R. A. *J. Phys. Chem.* **1994**, *98*, 8310.

(18) Bunte, S. W.; Chabalowski, C. F.; Wittig, C.; Beaudet, R. A. *J. Chem. Phys.* **1993**, *97*, 5864.

(19) Bunte, S. W.; Miller, J. B.; Huang, Z. S.; Verdasco, J. E.; Wittig, C. Beaudet, R. A. *J. Chem. Phys.* **1992**, *96*, 4140.

(20) Jäger, W.; Xu, Y.; Gerry, M. C. L. *J. Phys. Chem.* **1993**, *97*, 3685.

(21) Dutton, C.; Sazonov, A.; Beaudet, R. A. *J. Phys. Chem.* **1996**, *100*, 17772.

(22) Kroto, H. W. *Molecular Rotational Spectra*; Dover: New York, 1992; p 118.

(23) Hehre, W. J.; Ditchfield, R.; Pople, J. A. *J. Chem. Phys.* **1972**, *56*, 2257.

(24) Andzelm, J.; Klobukowski, M.; Radzio-Andzelm, E. *J. Comput. Chem.* **1984**, *5*, 146.

(25) Boys, S. F.; Bernardy, F. *J. Mol. Phys*, **1970**, *19*, 553.

(26) . Frisch, M. J.; Trucks, G. W.; Schlegel, H. B.; Gill, P. M. W.; Johnson, B. G.; Wong, M. W.; Foresman, J. B.; Robb, M. A.; Head-Gordon, M.; Replogle, E. S.; Gomperts, R.; Andres, J. L.; Raghavachari, K.; Binkley, J. S.; Gonzalez, C.; Martin, R. L.; Fox, D. J.; Defrees, D. J.; Baker, J.; Stewart, J. J. P.; Pople, J. A. *Gaussian 92/DFT*, Revision G.3; Gaussian: Pittsburgh, PA, 1993.

(27) Hobza, P.; Zahradnik, R. *Intermolecular Complexes*; Elsevier: New York, 1988; p 66.

(28) Stogryn, D. E.; Stogryn, A. P. *Mol. Phys.* **1966**, *11*, 371.

(29) Archibong, E. F. Thakkar, A. J. *Chem. Phys. Lett.* **1993**, *201*, 485.

(30) Dutton, C.; Beaudet, R. A. *J. Phys. Chem. A*, in press.

(31) Jucks, K. W.; Huang, Z. S.; Miller, R. E.; Fraser, G. T.; Pine, A. S.; Lafferty, W. J. *J. Chem. Phys.* **1987**, *88*, 2185.

(32) Huang, Z. S.; Miller, R. E. *J. Chem. Phys.* **1988**, *89*, 5408.

(33) Herzberg, G. *Molecular Spectra and Molecular Structure II*; Van Nostrand-Reinhold: New York, 1991; p 394.

(34) Fraser, G. T.; Leopold, K. R.; Klemperer, W.; *J. Chem. Phys.* **1984**, *80*, 1423.

(35) Hinds, K.; Legon, A. C. *Chem. Phys. Lett.* **1995**, *240*, 467.